symmetry

MDPI

Article

Spatial Kinetic Modeling of Crowd Evacuation: Coupling Social Behavior and Infectious Disease Contagion

Juan Pablo Agnelli [1,2,†], Claudio Armas [1,2,†] and Damián A. Knopoff [1,3,*,†]

[1] Centro de Investigaciones y Estudios en Matemática (CIEM), CONICET, Medina Allende s/n, Córdoba 5000, Argentina; jpagnelli@unc.edu.ar (J.P.A.); claudio.armas@unc.edu.ar (C.A.)
[2] FaMAF, Universidad Nacional de Córdoba, Medina Allende s/n, Córdoba 5000, Argentina
[3] Faculty of Engineering, University of Deusto, Av. de las Universidades 24, 48007 Bilbao, Spain
* Correspondence: d.knopoff@deusto.es
† These authors contributed equally to this work.

Abstract: This paper introduces a kinetic model of crowd evacuation from a bounded domain, integrating social behavior and contagion dynamics. The model describes the spatial movement of individuals in a crowd, taking into account interactions with other people and the geometry of the environment. Interactions between healthy and infectious individuals can lead to disease transmission and are considered. The approach is grounded in the kinetic theory of active particles, where the activity variable represents both the infectious disease status of individuals (e.g., susceptible, infected) and the psychological state of pedestrians, including contagion awareness. Varying awareness levels influence individual behavior, leading to more cautious movement patterns, potentially reducing the overall infection rate. The performance of the model is evaluated through a series of numerical simulations. Different scenarios are examined to investigate the impact of awareness levels on pedestrian behavior, infectious disease spread, and evacuation times. Additionally, the effects of population immunization and individual contagion awareness are assessed to determine the most effective strategy for reducing infections. The results provide valuable insights into targeted strategies to mitigate contagion.

Keywords: kinetic theory; crowd dynamics; disease contagion; awareness

Academic Editors: Michel Planat and Linjie Liu

Received: 25 November 2024
Revised: 1 January 2025
Accepted: 13 January 2025
Published: 15 January 2025

Citation: Agnelli, J.P.; Armas, C.; Knopoff, D.A. Spatial Kinetic Modeling of Crowd Evacuation: Coupling Social Behavior and Infectious Disease Contagion. *Symmetry* **2025**, *17*, 123. https://doi.org/10.3390/sym17010123

1. Introduction

Recent global health crises, such as the COVID-19 pandemic, have underscored the critical importance of understanding and modeling the dynamics of infectious disease spread in crowded environments [1]. Traditional epidemiological models, while effective in many scenarios, often lack the spatial and behavioral granularity needed to accurately predict disease transmission in specific settings, such as during evacuations in indoor venues. For instance, research such as that reported in [2,3] provides some hints to understand the spatial propagation of a disease. In addition, ref. [4] addresses the influence of travel with a focus on geographical dimensions, while the review [5] provides important insights into the wide variety of infectious diseases that may be considered in such settings.

This paper builds upon the spatial kinetic model of crowd evacuation dynamics for infectious disease contagion proposed by Agnelli et al. [6] The kinetic theory of active particles (KTAP) has been extensively utilized to study large systems of multiple interacting living entities [7–10]. In this theory, interactions deviate from the classical mechanics of inert matter, as they do not conserve momentum and energy and are not reversible. The KTAP addresses the conceptual challenges of studying living matter. Unlike physical systems of inert matter, biological phenomena cannot be studied using the same foundational theories and causality principles. This distinction has been highlighted by scientists developing a mathematical theory of living systems, as in [11–13].

Coupling crowd dynamics and disease propagation requires a multiscale approach due to the complex interactions at different levels [14,15]. At the microscopic scale, individual behaviors and interactions are modeled using ordinary differential equations, capturing the detailed dynamics of each person. At the macroscopic scale, the system is described by averaged quantities such as density and velocity, using conservation laws to model the overall flow of the crowd. The mesoscopic scale, central to the kinetic theory, bridges these two by describing the probability distribution of individuals' states and incorporating nonlocal, nonlinear interactions through tools from statistical mechanics and game theory.

The original model by Agnelli et al. [6] integrates the movement of individuals within a bounded domain, considering interactions with the environment and among individuals as in [16], but also including the spread of an infectious disease. This model employs a kinetic theory approach, utilizing game theory to describe the decision-making processes of individuals as they navigate towards exits while avoiding high-density areas and potential infection sources. However, the model does not explicitly account for the role of contagion awareness, namely, how individuals' knowledge and perception of infection risk influence their behavior and, consequently, the overall dynamics of disease spread.

This study extends the models by Agnelli et al. [6,16] by introducing a novel microscopic variable that accounts for contagion awareness and its propagation among individuals in a crowd. Incorporating contagion awareness into the model is crucial for several reasons. For instance, awareness can significantly alter individual behavior, leading to more cautious movement patterns and potentially reducing the overall infection rate. In addition, the propagation of awareness itself can be dynamic, influenced by factors such as communication among individuals, visible symptoms, and public health messaging. By modeling these aspects, deeper insights into the interplay between human behavior and disease transmission can be gained, which is essential for designing effective intervention strategies. Some hints in this line of research can be found in the contribution by Quaini et al. [17], where a crowd dynamics model that incorporates the influence of emotional contagion, specifically fear, on pedestrian movement and behavior is presented. It is worth stressing that the awareness level is generally referred to as threshold [16] or to the average levels [17] and this paper generalizes these ideas by introducing a time-evolving heterogeneously distributed variable, like the mechanical or disease-related ones. More recently, papers [18,19] study how awareness and stress are spread using a macroscopic and a microscopic approach, respectively. Readers are referred to [20] and references therein, where a broad vision of the behavior of human crowds is presented. The tools of learning-from-data and artificial intelligence have lately been included in the field of the kinetic modeling of the behavior of crowds as in [21,22]. The novelty of this present paper is the multiscale nature of the model: interactions are studied at the microscale, the model is mesoscopic, and emerging macroscopic behaviors for disease dynamics and pedestrian awareness are obtained.

The structure of this paper is as follows: Section 2 presents the extended mathematical model, detailing the incorporation of the contagion awareness variable. Section 3 presents the numerical methods used for simulation and the setup of the case studies, as well as the results of the simulations, highlighting the impact of contagion awareness on pedestrian behavior, infectious disease spread, and evacuation times, and discussing the main results. Finally, Section 4 concludes the paper with a summary of the key findings, limitations of the model, and potential directions for future research.

2. The Mathematical Model

This section derives the model coupling crowd movement within a bounded domain with disease contagion and awareness spread.

2.1. Functional Subsystems, Microscopic Variables, and Characterization of the Domain

Let $\Omega \subset \mathbb{R}^2$ be a bounded domain. Consider a large system of pedestrians, regarded as active particles, moving in Ω. The domain has the following features:

- The boundary $\partial\Omega$, including the exit zone $E \subset \partial\Omega$. Note that E could be the finite union of disjoint sets, i.e., the domain may have several exit zones. For instance, in Figure 1 there are two exits E_1 and E_2.
- The remainder of the boundary is an impenetrable wall $W \subset \partial\Omega$ (see Figure 1).
- For simplicity, the domain Ω is assumed to be convex.
- The domain Ω is characterized by an environmental quality parameter $\alpha \in [0, 1]$. The value of α ranges from 0, representing the most unfavorable conditions that force pedestrians to stop, to 1, representing ideal conditions that permit high-speed pedestrian movement.

Remark 1. *Parameter α can represent features such as signaling, lighting, existence of obstacles or fire, etc. For more details see [16]. Although internal obstacles are not considered, they can be added via a simple technical generalization of the model, as shown in reference [23].*

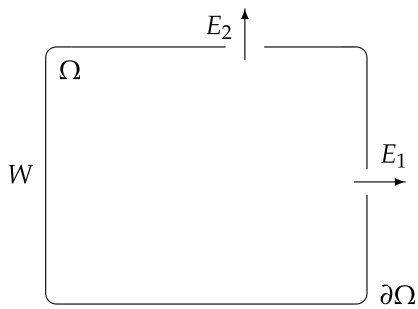

Figure 1. The geometric shape of the bounded domain Ω with boundary $\partial\Omega = W \cup E_1 \cup E_2$.

To study the movement of pedestrians within the domain Ω, let us introduce and describe their microscopic state. To do so, consider the ideas presented in [16], where a representation with continuous-discrete hybrid features is defined. In the following, the variables involved in our model are detailed:

- The position $\mathbf{x} = (x, y) \in \Omega$ is assumed to be a continuous variable.
- The velocity $\mathbf{v}$, expressed in polar coordinates as $\mathbf{v} = v(\cos\theta, \sin\theta)$, is modeled with a continuous speed component v that evolves deterministically over time and space, influenced by macroscopic effects. In contrast, the direction of velocity θ is treated as a discrete variable, exhibiting a heterogeneous distribution among pedestrians, with possible values restricted to the set

$$I_\theta = \left\{ \theta_i = \frac{i-1}{N_\theta} 2\pi \,:\, i = 1, \ldots, N_\theta \right\},$$

  with cardinal N_θ.
- A disease-related state given by a categorical variable in the set I_λ with cardinal N_λ. The set I_λ depends on the case under study. Two examples presented in [6] are $I_\lambda = \{S, E, I, R\}$ with $N_\lambda = 4$ (each class S , E, I, and R corresponds to susceptible, exposed, infected, and recovered, respectively) and $I_\lambda = \{S, E, I, R, V\}$ with $N_\lambda = 5$ (where V corresponds to a vaccinated class).

- A state that represents a pedestrian's level of awareness about the risk of contracting an infectious disease. This variable is denoted by ξ and a discrete set of levels is defined,
$$I_\xi = \{\xi_k \in [0,1] : k = 1, ..., N_\xi\}.$$
The lowest level ξ_1 corresponds to the state in which a pedestrian is not aware of a possible contagion (their only objective is to reach the exit). On the other hand, the highest level ξ_{N_ξ} corresponds to the state in which a pedestrian is absolutely aware of a possible contagion and, therefore, their priority will be to avoid high densities. It is worth stressing that even in that case, pedestrians do not lose the objective of leaving the room.

Remark 2. *The term functional subsystem (FS) will be used to identify groups of particles sharing a common micro-state. For instance, the function $(\lambda_j, \xi_k, \theta_i)$-FS refers to those active particles belonging to the λ_j-class, having a level of awareness ξ_k and moving with direction θ_i. If the case under study requires it, functional subsystems for a micro-state concerning a single variable can be represented, e.g., ξ_k-FS denotes those active particles who have a level of awareness ξ_k.*

The general state of active particles is given by the distribution function $f_{jki}(t, \mathbf{x}) = f(t, \mathbf{x}, \lambda_j, \xi_k, \theta_i)$. This is interpreted as the number of particles that, at time t, are located in $\mathbf{x}$, are carriers of the disease-related state λ_j and of a level of awareness ξ_k, and move with direction θ_i.

As in [6], the physical dimensions are removed by nondimensionalization, so that the local density can reach a maximum of 1 under normal conditions. In this way, the local density is given by the zero-th order moment:

$$\rho(t, \mathbf{x}) = \sum_{j=1}^{N_\lambda} \sum_{k=1}^{N_\xi} \sum_{i=1}^{N_\theta} f_{jki}(t, \mathbf{x}).$$

Computing some marginal moments, let us obtain the local density of certain FSs. For instance, the local density of individuals belonging to the λ_j-class is

$$\rho^{\lambda_j}(t, \mathbf{x}) = \sum_{k=1}^{N_\xi} \sum_{i=1}^{N_\theta} f_{jki}(t, \mathbf{x}),$$

and the total population belonging to the λ_j-FS within the domain at time t is given by

$$\int_\Omega \rho^{\lambda_j}(t, \mathbf{x}) d\mathbf{x}. \tag{1}$$

2.2. Mathematical Structure

Following the models developed in [6,16], interactions of pedestrians with the environment and with all other pedestrians are taken into account. For our large system of active particles that interact, subdivided into functional subsystems $N_\lambda \times N_\xi \times N_\theta$, the mathematical structure is obtained by a suitable balance of particles in the elementary volume of the microscopic states space. The net flow into this volume is attributed to the combined effects of transport and interactions and is modeled by the following equation:

$$\partial_t f_{jki}(t, \mathbf{x}) + \mathrm{div}_\mathbf{x}(\mathbf{v}_i[\rho](t, \mathbf{x}) f_{jki}(t, \mathbf{x})) = \mathcal{J}_{jki}[f](t, \mathbf{x}), \tag{2}$$

for $j = 1, \ldots, N_\lambda$, $k = 1, \ldots, N_\xi$ and $i = 1, \ldots, N_\theta$, and where $\mathbf{v}_i[\rho] = v[\rho](\cos\theta_i, \sin\theta_i)$. The left-hand term models the transport of particles, while the right-hand term $\mathcal{J}_{jki}[f]$ represents the net balance for those particles in the $(\lambda_j, \xi_k, \theta_i)$-FS due to interactions.

In this study, it is assumed that the interaction dynamics, represented by the nonlinear term $\mathcal{J}_{jki}$ in Equation (2), are determined by the following features:

1. moving towards the exit;
2. avoiding collision with walls;
3. moving towards less congested areas;
4. attraction to follow the main stream;
5. disease contagion;
6. pedestrian awareness.

Note the distinction between the first two items, which are related to essentially geometric characteristics of the domain, and the subsequent four, which take into consideration that pedestrian behavior is heavily impacted by the presence of other pedestrians. Thus, the right-hand term in Equation (2) that models the interaction dynamics is split into two terms

$$\mathcal{J}_{jki}[f] = \mathcal{J}_i^G[f] + \mathcal{J}_{jki}^P[f],$$

where $\mathcal{J}_i^G$ accounts for the difference between the gain and the loss of particles moving in direction θ_i, due only to the influence of the geometrical features, and $\mathcal{J}_{jki}^P$ accounts for the balance due to interactions between particles belonging to the $(\lambda_j, \xi_k, \theta_i)$-FS with the other subsystems.

Interactions can modify the internal state of the interacting pedestrians. Here, it is assumed that interactions between pedestrians and the environment (given by items 1 and 2) may modify the walking direction θ of the pedestrian. Interactions between pedestrians (related to items 3 to 6) can modify the walking direction θ of the pedestrian, but can also modify the disease-related state λ and the awareness level ξ (see Figure 2 for a schematic representation and Section 2.3 for a detailed description).

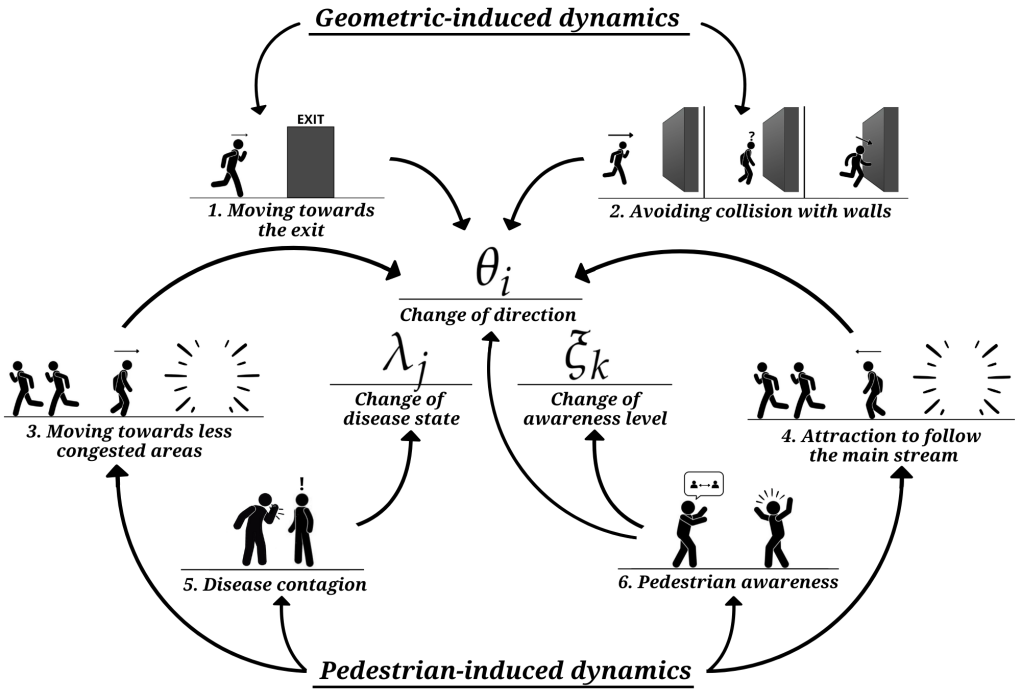

Figure 2. Schematic representation of the features that are considered in the model and the microscopic variables over which they have influence.

In order to model changes in the internal state, probabilistic rules are used. Taking inspiration from [6], the following transition probabilities are defined:

- $\mathcal{A}_h(i)$ with $h, i = 1, ..., N_\theta$ models changes in the velocity direction. The quantity $\mathcal{A}_h(i)$ is the probability that an individual moving with direction θ_h adjusts its direction into θ_i as a consequence of the domain geometry (e.g., walls or exit doors).
- $\mathcal{B}^{rql}_{sph}(j,k,i)$ with $s,r,j = 1,\dots,N_\lambda$, $p,q,k = 1,\dots,N_\xi$ and $h,l,i = 1,\dots,N_\theta$ models inter-pedestrian interactions. In this study, three different types of interactions between pedestrians are assumed, which are modeled by the following transition probabilities:
  - $\mathcal{B}^1_{sr}(j)$ describes the probability that an individual with disease state λ_s undergoes a transition into the disease state λ_j as a consequence of an interaction with an individual with disease state λ_r,
  - $\mathcal{B}^2_{pq}(k)$ represents the probability that an individual with level of awareness ξ_p changes to level ξ_k as a consequence of an interaction with an individual with level of awareness ξ_q, and
  - $\mathcal{B}^3_{hl}(i)$ denotes the probability that a pedestrian walking with direction θ_h changes its direction into θ_i after an interaction with a pedestrian moving with direction θ_l. In Section 2.3.2, it will be shown that this transition also depends indirectly on the awareness level ξ_p of the individual.

Then, the compact form of the inter-pedestrian interactions transition probability is given by the product

$$\mathcal{B}^{rql}_{sph}(j,k,i)[\rho] = \mathcal{B}^1_{sr}(j) \times \mathcal{B}^2_{pq}(k) \times \mathcal{B}^3_{hl}(i),$$

and represents the probability that a pedestrian with infectious state λ_s, level of awareness ξ_p, and moving with direction θ_h undergoes a transition into the infectious state λ_j, level of awareness ξ_k, and direction θ_i after an interaction with a pedestrian with state λ_r, level of awareness ξ_q, and moving with direction θ_l.

Remark 3. *Notice that the symbol $\mathcal{A}$ represents transitions depending only on the geometry of the domain, while $\mathcal{B}$ considers interactions among pedestrians.*

The transition probabilities $\mathcal{A}$ and $\mathcal{B}$ satisfy

$$\sum_{i=1}^{N_\theta} \mathcal{A}_h(i) = 1, \qquad \forall\, h = 1, ..., N_\theta,$$
$$\sum_{j=1}^{N_\lambda}\sum_{k=1}^{N_\xi}\sum_{i=1}^{N_\theta} \mathcal{B}^{rql}_{sph}(j,k,i) = 1, \qquad \forall\, s,r = 1,...,N_\lambda,\ \forall\, p,q = 1,...,N_\xi,\ \forall\, h,l = 1,...,N_\theta,$$

guaranteeing the conservation in the number of total pedestrians.

Taking into account all the previously defined terms, Equation (2) can be expressed as

$$\begin{aligned}
\partial_t f_{jki}(t,\mathbf{x}) + \mathrm{div}_{\mathbf{x}}(\mathbf{v}_i[\rho](t,\mathbf{x}) f_{jki}(t,\mathbf{x})) &= \mathcal{J}^G_i[f](t,\mathbf{x}) + \mathcal{J}^P_{jki}[f](t,\mathbf{x}) \\
&= \mu[\rho(t,\mathbf{x})]\left(\sum_{h=1}^{N_\theta} \mathcal{A}_h(i) f_{jkh}(t,\mathbf{x}) - f_{jki}(t,\mathbf{x})\right) \\
&\quad + \eta[\rho(t,\mathbf{x})]\left(\sum_{s,r=1}^{N_\lambda}\sum_{p,q=1}^{N_\xi}\sum_{h,l=1}^{N_\theta} \mathcal{B}^{rql}_{sph}(j,k,i)[\rho] f_{sph}(t,\mathbf{x}) f_{rql}(t,\mathbf{x}) - f_{jki}(t,\mathbf{x})\rho(t,\mathbf{x})\right)
\end{aligned} \tag{3}$$

for $j = 1,\dots,N_\lambda$, $k = 1,\dots,N_\xi$ and $i = 1,\dots,N_\theta$. As mentioned above, the term $\mathcal{J}^G_i$ represents the net effect of the geometrical influences on particles moving in direction θ_i, capturing the difference between the particle gain and loss. In contrast, $\mathcal{J}^P_{jki}$ accounts for the balance arising from the binary interactions among particles. The expressions μ and η are the interaction rates modeling the frequency of interactions with the geometry of the environment and with other pedestrians, respectively. Both terms depend on the local density ρ and weight the relative importance of $\mathcal{J}_i^G$ and $\mathcal{J}_{jki}^P$. A more precise definition will be presented in the next section.

2.3. Modeling the Interactions

Let us now concentrate on shaping the interactions that result in the term of the right-hand side of Equation (3). Let us differentiate two types of dynamics: (i) dynamics induced by the shape of the environment, and (ii) dynamics induced by interactions between pedestrians. The first type is related to description of interactions between a pedestrian and the geometry of the domain where the dynamics occurs and this type of interaction can produce a change in the walking direction of the pedestrian. The second type of dynamics is associated with binary interactions between pedestrians. This type of interaction may produce a transition into the disease state, a change in the level of awareness, and also change in the walking direction.

Before starting to describe the two types of dynamics mentioned previously, it is necessary to define three types of particles:

- ***test particles*** with micro-state $(\mathbf{x}, \lambda_j, \xi_k, \theta_i)$, which are representative of the entire system;
- ***field particles*** with micro-state $(\mathbf{x}, \lambda_r, \xi_q, \theta_l)$, whose presence triggers the interactions of the candidate particles, and;
- ***candidate particles*** with micro-state $(\mathbf{x}, \lambda_s, \xi_p, \theta_h)$, that can probabilistically transition to the state of test particles through interactions with field particles or the environment.

2.3.1. Dynamics Induced by the Shape of the Environment

Following the ideas presented in [16], the geometry of the domain is assumed to have an influence on the pedestrian's choice of his/her walking direction and this influence is due to:

- *Trend to move toward the exit.* Pedestrians in an evacuation may try to reach the exit by moving through the shortest path from where they are currently located. Given a candidate particle at the point $\mathbf{x}$, its distance to the exit is defined as

$$d_E(\mathbf{x}) = \min_{\mathbf{y} \in E} \|\mathbf{x} - \mathbf{y}\|,$$

  where $\|\cdot\|$ denotes the Euclidean norm in $\mathbb{R}^2$, and the unitary vector is considered to be $\vec{v}(\mathbf{x})$, pointing from $\mathbf{x}$ to the exit (see Figure 3a).
- *Trend to avoid collision with walls.* A pedestrian at position $\mathbf{x}$ and moving in direction θ_h that does not point towards the exit, will collide with the wall at a point $\mathbf{x}_W(\mathbf{x}, \theta_h)$ and a distance $d_W(\mathbf{x}, \theta_h)$ from him/her, unless he/she changes direction (see Figure 3b). Thus, to avoid this collision, the pedestrian must select a suitable new direction. Building on the model presented in [16], define the unit tangent vector $\vec{\tau}(\mathbf{x}, \theta_h)$ along the boundary $\partial\Omega$ at $\mathbf{x}_W$, oriented to guide the particle closer to the exit.

The two aforementioned trends are related to essentially geometric features of the domain, meaning that candidate particles take into account the presence of doors or walls. The modeling approach is based on the following assumptions:

(A1) The trend to the exit increases as pedestrians get closer to it.
(A2) Pedestrians experience a stronger influence to avoid the wall as they approach it.

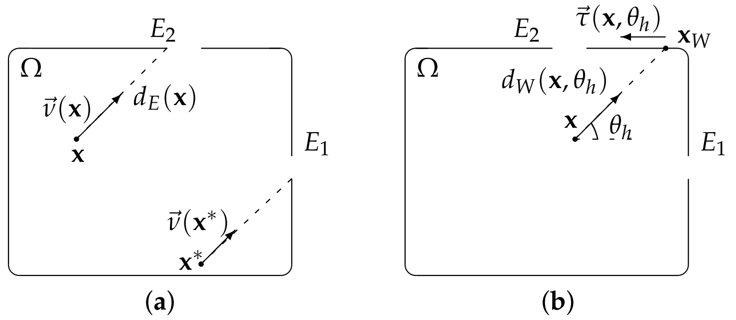

Figure 3. (**a**) For a particle situated at **x**, the distance to the nearest exit is denoted by $d_E(\mathbf{x})$, and the vector pointing from **x** to the exit is represented by $\vec{v}(\mathbf{x})$. (**b**) A particle moving in direction θ_h from the point **x** is expected to collide with the wall at $\mathbf{x}_W$, then it calculates the tangent direction to the wall that would take it toward the exit.

Pedestrians may respond differently when faced with the same particular circumstance. That is, every pedestrian, depending on his/her position, has the ability to employ a different strategy to choose in which direction to move, either avoiding the walls or reaching the exit. This heterogeneity can be efficiently modeled using a probabilistic approach. Specifically, to model the dynamics induced by the shape of the environment consider the following two terms:

- The interaction rate $\mu[\rho]$ represents the frequency at which candidate particles interact with the domain boundary. It is assumed that μ decreases as the local density increases, because lower densities enable pedestrians to more easily perceive the presence of walls and doors. Based on this idea, it is assumed that $\mu[\rho] \sim 1-\rho$.
- The transition probability $\mathcal{A}_h(i)$ is the probability that a candidate particle moving with direction θ_h adjusts its direction into that of the test particle θ_i, induced by the presence of walls and exit areas.

The modeling approach postulates that pedestrians probabilistically change their direction only to an adjacent direction (clockwise or counterclockwise) in the discrete set I_θ. Consequently, a candidate h-particle may transition to the states h_1, $h+1$, or remain in its current state h. Notably, for $h=1$, θ_{h-1} is equivalent to θ_{N_θ}, whereas for $h=N_\theta$, θ_{h+1} is equivalent to θ_1.

The set of all transition probabilities $\mathcal{A}=\{\mathcal{A}_h(i)\}_{h,i=1,\dots,N_\theta}$ forms the so-called *table of games* that models the game played by active particles when they interact with the environmental geometry.

According to assumptions (A1)–(A2), define the vector

$$\vec{\omega}_G(\mathbf{x},\theta_h) = [1-d_E(\mathbf{x})]\,\vec{v}(\mathbf{x}) + [1-d_W(\mathbf{x},\theta_h)]\,\vec{\tau}\,(\mathbf{x},\theta_h),$$

whose direction θ_G is the ***geometrical preferred direction***, indicating the ideal direction that a pedestrian should take in order to reach the exit and avoid the walls in the most efficient manner.

Due to the discretization of directions, an h-particle updates its direction by selecting the option closest to θ_G from the three permissible directions: θ_{h-1}, θ_h, and θ_{h+1}. The table of games $\mathcal{A}$ can be represented in compact form as follows:

$$\mathcal{A}_h(i) = \beta_h(\alpha)\delta_{s,i} + [1-\beta_h(\alpha)]\delta_{h,i}, \quad i = h-1, h, h+1,$$

where

$$s = \underset{j\in\{h-1,h+1\}}{\arg\min}\,\{d(\theta_G,\theta_j)\},$$

$$d(\theta_*, \theta^*) = \begin{cases} |\theta_* - \theta^*|, & \text{if} \quad |\theta_* - \theta^*| \le \pi, \\ \\ 2\pi - |\theta_* - \theta^*|, & \text{if} \quad |\theta_* - \theta^*| > \pi, \end{cases}$$

$\delta_{j,i}$ denotes the Kronecker delta function, and the coefficient β_h, proportional to the parameter α, is introduced to describe the fact that even in the case that the geometrical preferred direction θ_G is close to θ_h, a transition may occur, and the more distant the two states are, the more probable is this transition:

$$\beta_h(\alpha) = \begin{cases} \alpha, & \text{if} \quad d(\theta_h, \theta_G) \ge \Delta\theta, \\ \\ \alpha \frac{d(\theta_h, \theta_G)}{\Delta\theta}, & \text{if} \quad d(\theta_h, \theta_G) < \Delta\theta, \end{cases}$$

where $\Delta\theta = 2\pi/n$. Notice that if $\theta_G = \theta_h$, then $\beta_h = 0$ and $\mathcal{A}_h(h) = 1$, meaning that a pedestrian keeps the same direction, at least due to the influence of the geometrical features, with probability 1.

2.3.2. Dynamics Induced by Interactions Between Pedestrians

Binary interactions, at time t and position $\mathbf{x}$, involve the interplay of test, candidate, and field particles. As a result of these interactions, a candidate particle may probabilistically transition to the state of the test particle, under the influence of field particles, while the test particle may lose its state.

To model the dynamics induced by interaction between pedestrians, consider the following two terms:

- The *interaction rate* $\eta[\rho]$ that defines the number of binary encounters per unit time. If the local density increases, then the interaction rate also increases.
- The transition probability $\mathcal{B}_{sph}^{rql}(j,k,i) = \mathcal{B}_{sr}^{1}(j) \times \mathcal{B}_{pq}^{1}(k) \times \mathcal{B}_{hl}^{3}(i)$ that represents the probability that a pedestrian with infectious state λ_s, level of awareness ξ_p, and moving with direction θ_h undergoes a transition into infectious state λ_j, level ξ_k, and direction θ_i after an interaction with a pedestrian with state λ_r, level of awareness ξ_q, and moving with direction θ_l.

Note that interaction between pedestrians can produce: (i) a transition into the disease state λ, (ii) a change in the level of awareness ξ of the particles involved, and (iii) a change in the walking direction θ, which, in turn, is affected by the level of awareness. In the following, each interaction and its outcome will be analyzed in detail.

(I) Interactions can modify the state related to the disease.

Every individual possesses a unique internal micro-state that reflects their health status regarding an infectious disease. To simplify the analysis, let us start by considering a basic scenario where the population is segmented into four non-overlapping groups (which can be regarded as functional subsystems of our theoretical framework). Notably, we introduce $I_\lambda = \{S, E, I, R\}$, where S, E, I, and R represent susceptible, exposed, infectious, and recovered individuals, respectively.

The time scale for evacuation from a room is relatively short compared to the period of time it takes for an individual to become contagious after infection. As a result, it is crucial to incorporate the disease latency period into our model, including the exposed compartment E. When a susceptible individual comes into contact with an infectious one, she may become infected but will not transmit the disease during the latency period, until transitioning from E to I. This transition typically occurs *after* evacuation, and our focus lies in tracking and understanding the contagion dynamics *during* the evacuation process.

The dynamics of an SEIR model can be described by the following reaction scheme:

$$\begin{array}{ccc} S+I & \xrightarrow{i_{r_S}} & E+I \\ E & \xrightarrow{p_{EI}} & I \\ I & \xrightarrow{p_{IR}} & R, \end{array} \tag{4}$$

where permanent waning immunity is assumed (thus, individuals in the R compartment maintain their immune status and do not transition back to the susceptible compartment S).

In this framework, contagion is assumed to follow the law of mass action, with a specified infection rate i_{r_S} that governs the transition of susceptible individuals to the exposed state upon interaction with an infected individual. The transitions from the exposed to the infectious state, and subsequently from the infectious to the recovered state, are compartment-size dependent, with p_{EI} and p_{IR} representing the respective transition rates. However, due to the relatively short time scale involved in evacuating a room, our analysis focuses on the evacuation time interval. Consequently, our table of games only accounts for the first transition in Equation (4). Thus, rates p_{EI} and p_{IR} can be neglected and the only non-trivial entry in the table of games for contagion dynamics takes the form $\mathcal{B}^1_{SI}(E) = i_{r_S}$, while all the other interactions are unaffected.

Incorporating a vaccinated class provides valuable insights, as will be demonstrated in subsequent numerical experiments. To achieve this, the model is expanded to include a compartment V representing susceptible individuals who, despite vaccination, can still contract the infection but with a lower rate. In an ideal scenario of a perfectly effective vaccine, the infection rate would be zero; however, in general, a non-negative value $i_{r_V} \leq i_{r_S}$ is assumed.

The reaction scheme for the so-called SEIRV model is:

$$\begin{array}{ccc} S+I & \xrightarrow{i_{r_S}} & E+I \\ V+I & \xrightarrow{i_{r_V}} & E+I \\ E & \xrightarrow{p_{EI}} & I \\ I & \xrightarrow{p_{IR}} & R, \end{array}$$

and the transition probability densities shall be changed accordingly by adding the non-trivial entry $\mathcal{B}^1_{VI}(E) = i_{r_V}$.

(II) *Interactions can modify the level of awareness.*

A binary interaction between pedestrians can modify their awareness level. In more detail, let us consider the different kinds of interactions that can occur between a candidate pedestrian with awareness level ξ_p and a field pedestrian with awareness level ξ_q:

- If two pedestrians with the same awareness level interact, then both of them remain at the same level.
- If two pedestrians with different levels of awareness interact, then one pedestrian can influence the other and, as a result, the pedestrian having a lower awareness level may increase her level, while the one with a higher level may face a decrease in her level of awareness.

Notice that an individual with awareness level ξ_1 cannot decrease her level since she is at the lowest possible level. Similarly, an individual with awareness level ξ_{N_ξ} cannot increase her level, which is already at the highest possible stage. Therefore, after an interaction between a candidate particle with awareness level ξ_p and a field particle with awareness level ξ_q, the possible levels to which the candidate particle can change are given by the following set of indices:

$$\mathrm{Idx}_p = \begin{cases} \{1,2\} & \text{if } p = 1 \\ \{N_\xi - 1, N_\xi, N_\xi + 1\} & \text{if } 2 \leq p \leq N_\xi - 1 \\ \{N_\xi - 1, N_\xi\} & \text{if } p = N_\xi. \end{cases}$$

Taking all the previous assumptions into account, the transition probability $\mathcal{B}^2$ is given by

$$\mathcal{B}^2_{pq}(k) = \varphi_{pq}\delta_{m,k} + (1 - \varphi_{pq})\delta_{p,k}, \quad k \in \mathrm{Idx}_p,$$

where m is defined as

$$m = \arg\min_{j \in \mathrm{Idx}_p} \{|\xi_j - \xi_q|\},$$

φ_{pq} is given by

$$\varphi_{pq} = \chi|\xi_p - \xi_q|, \tag{5}$$

and where $\chi \in [0,1]$ is a parameter related to the influence between pedestrians. A larger χ value indicates a greater probability of changing the state ξ_p, meaning the candidate particle is largely influenced by a field particle. Conversely, a lower χ value leads to a reduced probability, meaning that the candidate particle is not much influenced by a field particle.

(III) Interactions can modify the walking direction.

Following the model presented in [16], pedestrians, induced by interaction with other pedestrians, may decide to change their walking direction taking into account the combination of the following causes:

- *Tendency to move towards less congested areas.* A candidate particle at $\mathbf{x}$, moving with direction θ_h, could decide, under the influence of his/her level of awareness ξ_p, to change direction by moving towards less congested areas. This direction is denoted by the unitary vector $\vec{\gamma}(\theta_h, \rho)$ and can be computed by choosing the direction that gives the minimal directional derivative of the density ρ at the point $\mathbf{x}$.
- *Tendency to follow the stream.* A candidate pedestrian, moving with direction θ_h and level of awareness ξ_p, that interacts with a field pedestrian may decide to follow him/her and, in consequence, adopt a new velocity direction. The unitary vector $\vec{\sigma}_l = (\cos\theta_l, \sin\theta_l)$ describes the movement of the field particle moving with direction θ_l.

Notice that the two tendencies take into account that pedestrian behavior is affected by that of others. Specifically, a candidate pedestrian can scan its environment to select, at each moment and position, an appropriate direction that will prevent it moving into congested areas. On the other hand, interaction with a field pedestrian will cause it to try to bring its direction closer to that of the latter.

Furthermore, the two preceding tendencies compete against one another. Put another way, higher densities will induce a higher tendency to look for less congested areas but, at the same time, to follow the stream. In fact, in [16], the authors introduce a parameter $\varepsilon \in [0,1]$ that reinforces one tendency or the other according to the particular situation to be modeled. The value $\varepsilon = 0$ represents a scenario where pedestrians solely prioritize the research of less congested areas. Conversely, $\varepsilon = 1$ corresponds to the situation where pedestrians exclusively follow the crowd.

This work proposes an alternative approach, where the two tendencies are related to the level of awareness of each pedestrian. Specifically, it is assumed that the higher the level of awareness of a candidate particle, the greater the probability of selecting a proper direction towards less congested areas. Conversely, the lower the level of awareness of a candidate particle, the greater the probability of following the stream. Therefore, differently from [6,16], where all pedestrians adopt the same strategy to follow the stream or to search for less congested areas, let us define a decreasing function $\psi : [0,1] \to [0,1]$, which will make every pedestrian in the ξ_p-FS have their own parameter $\varepsilon_p = \psi(\xi_p)$ depending on its level of awareness.

Therefore, the modeling approach is built upon the following assumptions:

(A3) The tendency to look for less congested areas depends on the local density and level of awareness of each active particle.

(A4) The tendency to follow the stream depends on the local density and level of awareness of each active particle.

Next, based on assumptions (A3) and (A4), the transition probability $\mathcal{B}^3$ can be modeled.

On the one hand, in order to change direction to move towards less congested areas consider how pedestrians react according to their perception of the density around them and choose the less congested direction among the three admissible ones. This direction can be computed for a candidate h-pedestrian in position $\mathbf{x}$ by taking

$$\ell = \ell(\theta_h, \rho(t,\mathbf{x})) = \underset{j\in\{h-1,h,h+1\}}{\arg\min} \{\partial_j \rho(t,\mathbf{x})\},$$

where $\partial_j \rho$ denotes the derivative of ρ in the direction θ_j. In this way, one has $\vec{\gamma}(\theta_h, \rho) = (\cos\theta_\ell, \sin\theta_\ell)$. Notice that in the case $h = 1$, $\theta_{h-1} = \theta_{N_\theta}$ holds, while in the case $h = N_\theta$, $\theta_{h+1} = \theta_1$ holds.

On the other hand, recall that $\vec{\sigma}_l$ denotes the vector pointing in the direction of the field particle.

Then, according to assumptions (A3)–(A4), define the vector

$$\vec{\omega}_P(\theta_h, \xi_p, \theta_l, \rho) = \psi(\xi_p)\,\vec{\sigma}_l + (1-\psi(\xi_p))\vec{\gamma}(\theta_h,\rho), \tag{6}$$

where the subscript P stands for pedestrians, and the direction θ_P of $\vec{\omega}_P$ is the ***interaction-based preferred direction***, calculated as a weighted average between the trend to follow the stream and the tendency to avoid crowded zones, under the influence of awareness level ξ_p. The proposed table of games is as follows:

$$\mathcal{B}^1_{hl}(i)[\rho] = \beta^p_{hl}(\alpha)\rho\delta_{n,i} + \left[1 - \beta^p_{hl}(\alpha)\rho\right]\delta_{h,i}, \quad i = h-1, h, h+1,$$

where n is defined as

$$n = \underset{j\in\{h-1,h+1\}}{\arg\min} \{d(\theta_P, \theta_j)\},$$

and β^p_{hl} is given by

$$\beta^p_{hl}(\alpha) = \begin{cases} \alpha, & \text{if} \quad d(\theta_h,\theta_P) \geq \Delta\theta \\ \alpha\frac{d(\theta_h,\theta_P)}{\Delta\theta}, & \text{if} \quad d(\theta_h,\theta_P) < \Delta\theta \end{cases} \qquad \text{for } p = 1,\ldots,N_\xi.$$

Remark 4. *Notice that the superscript p is implicit in the definition of β^p_{hl} since it impacts on the definition of the interaction preferred direction θ_P.*

2.4. Modeling the Velocity Modulus

The variation in pedestrian velocity is influenced by interactions among individuals. Pedestrians adjust their walking speed according to how crowded their surroundings are. It is assumed that the maximal reachable dimensionless velocity modulus $v_m =$

$v_m(\alpha)$ depends linearly on the quality of the environment, in such a way that $v_m(0) = 0$—any movement is hindered—and $v_m(1) = 1$—maximal speed is attainable when the environment is ideal. Additionally, it is assumed that the velocity is influenced by the locally perceived density. Specifically, the maximum velocity $v_m(\alpha)$ is maintained under low-density conditions (free-flow regime) until a critical density $\rho_c(\alpha)$ is reached, which can be experimentally measured. When the locally perceived density exceeds this threshold, the velocity modulus decreases to zero (slowdown zone). Within this zone, a polynomial-type dependence of the velocity modulus on the local density is chosen (see Section 3 of [16] for more details).

3. Numerical Results and Cases of Study

In this section, a set of numerical simulations of the model (2) is presented, aimed at exploring and analyzing the performance of the proposed model in different scenarios.

In order to solve numerically Equation (2), one must explicitly define the initial conditions $f_{jki}(0, \mathbf{x})$, for $j = 1, ..., N_\lambda$, $k = 1, ..., N_\xi$ and $i = 1, ..., N_\theta$, while the boundary conditions are not explicitly imposed but are induced by the nonlocal action over the pedestrians given by the term $\mathcal{J}_{jki}$. Indeed, pedestrians are induced to avoid walls according to the trends described in Section 2.3.1. To obtain a numerical solution of the system (2), a splitting method [24] is used, where the overall evolution operator is seen as the sum of simpler sub-problems describing different physical processes. Then, each sub-problem is solved by means of an appropriate scheme, and finally, all the pieces are attached together. In particular, Equation (2) is split into two sub-equations:

$$\partial_t f_{jki}(t, \mathbf{x}) + \mathrm{div}_{\mathbf{x}}(\mathbf{v}_i[\rho](t, \mathbf{x}) f_{jki}(t, \mathbf{x})) = 0, \tag{7}$$

and

$$\partial_t f_{jki}(t, \mathbf{x}) = \mathcal{J}_{jki}[f](t, \mathbf{x}), \tag{8}$$

for $j = 1, \ldots, N_\lambda$, $k = 1, \ldots, N_\xi$ and $i = 1, \ldots, N_\theta$. Notice that Equation (7) is a 2D homogeneous transport equation. Hence, to guarantee conservation of the total number of particles, a finite volume scheme to solve it is used (see [25–27] for more details on the implementation). On the other hand, Equation (8) is solved by means of a first-order Euler explicit method to go forward in time.

In all the numerical experiments of this section, Ω is assumed to be a square domain of side length 10 m with an exit door of width 2 m located on the right. This is the same domain used in [6,16,23]. The quality of the environment, α, is fixed for all case studies. It is assumed that $\alpha = 1$, so that each pedestrian has the possibility to reach her maximum permitted speed. Similarly, the interaction rates are fixed and equal to $\mu = 1 - \rho$ and $\eta = \rho$. Additionally, nondimensional quantities are obtained by referring to the spatial coordinates relative to the longest dimension of the domain $L = 10\sqrt{2}$ m, while the density and velocity modulus are referred to $\rho_M = 7\ \mathrm{m}^{-2}$ and $V_M = 2$ m/s, respectively, following the experimental values presented in [28]. From these values, one obtains the reference time $T_M = 5\sqrt{2}$ s. The set I_λ related to the disease state is given by

$$I_\lambda = \Big\{S, I, E, R, V\Big\}.$$

The infection rates $i_{r_S} = 0.1$ and $i_{r_V} = 0.01$ are kept fixed [6]. Note that contagion is considered only within the domain as the disease dynamics once individuals are outside the room are not monitored. Additionally, the set I_ξ related to the awareness level is defined as

$$I_\xi = \Big\{\xi_k = \frac{k-1}{3}, k = 1, ..., 4\Big\},$$

and parameter χ in Equation (5) related to the influence between pedestrians is fixed at $\chi = 0.7$. Finally, the set I_θ of possible velocity directions is given by

$$I_\theta = \left\{ \theta_i = \frac{i-1}{8} 2\pi,\, i = 1, \ldots, 8 \right\},$$

while the velocity modulus is assumed to depend on the perceived density and on the quality of the environment. In all the considered case studies, approximately 50 pedestrians initially move with direction θ_1. Thus, $f_{jki}(0, \mathbf{x}) = 0$, for $j = 1, \ldots, 5$, $k = 1, \ldots, 4$ and $i = 2, \ldots, 8$.

Recall that, according to Equation (1), the total number of pedestrians belonging to each infectious compartment within the domain Ω and at time t is given by

$$S(t) = \int_\Omega \rho^S(t, \mathbf{x}) d\mathbf{x}, \quad E(t) = \int_\Omega \rho^E(t, \mathbf{x}) d\mathbf{x},$$
$$I(t) = \int_\Omega \rho^I(t, \mathbf{x}) d\mathbf{x}, \quad R(t) = \int_\Omega \rho^R(t, \mathbf{x}) d\mathbf{x},$$

where $S(t)$, $E(t)$, $I(t)$, and $R(t)$ are the susceptible, exposed, infectious, and recovered populations within the domain, respectively. Note that contagion is considered only within the domain as the disease dynamics once individuals are outside the room are not monitored.

Similarly, the total number of pedestrians with awareness level ξ_k within the domain Ω and at time t is given by

$$\xi_k(t) = \int_\Omega \rho^{\xi_k}(t, \mathbf{x}) d\mathbf{x}, \quad k = 1, \ldots, 4. \tag{9}$$

In the following subsections, a selection of case studies is presented to understand and analyze the model performance under different scenarios. The model was numerically solved in MATLAB [29] following the splitting method described above. The first case study focuses on the influence of awareness levels on the overall dynamics. The second case study investigates which condition, aware or vaccinated, preponderates in leading to fewer infections. Finally, different functions ψ involved in the definition of the interaction-based preferred direction (6) are studied in the last case study.

3.1. Case Study 1: The Influence of Awareness Levels

This case study analyzes the influence of the state ξ on the evacuation process. The objective is to understand how this state affects pedestrian behavior and its subsequent consequences for the spread of infectious disease and evacuation times. Furthermore, the potential indirect influence of ξ on velocity magnitude is investigated. This study is particularly relevant in real-life scenarios, such as emergency evacuations during infectious disease outbreaks, where public awareness and behavior significantly impact both the efficiency of the evacuation and the control of disease spread. Eight different scenarios are analyzed in this first case study. Table 1 presents the different scenarios that are studied, showing the initial proportions of the involved populations related both to awareness and infectious levels, aiming to describe how effectively people adopted preventive measures (e.g., mask-wearing, social distancing) after awareness campaigns. In addition, the last column shows the definition of the function ψ that is used for each scenario, which for this case study is maintained as $\psi(\xi) = 1 - \xi$.

Table 1. Scenarios considered in Case Study 1. Initial proportions for awareness and infectious levels are shown, as well as the definition of function ψ.

Scenarios	Initial Proportion of Individuals (%) and Function ψ								
	ξ_1	ξ_2	ξ_3	ξ_4	S	I	E	V	$\psi(\xi)$
1	80	5	5	10	75	25	0	0	$1-\xi$
2	10	5	5	80	75	25	0	0	$1-\xi$
3	75	12.5	12.5	0	75	25	0	0	$1-\xi$
4	0	12.5	12.5	75	75	25	0	0	$1-\xi$
5	100	0	0	0	75	25	0	0	$1-\xi$
6	0	0	0	100	75	25	0	0	$1-\xi$
7	20	35	35	10	75	25	0	0	$1-\xi$
8	10	35	35	20	75	25	0	0	$1-\xi$

Let us first analyze the influence of awareness levels on pedestrians. Observe in Figure 4 that scenarios where a large percentage of pedestrians initially have the highest awareness level ξ_4 lead to fewer exposed individuals compared to scenarios that started with a large percentage at the level ξ_1. The analysis begins with scenarios where most of the population initiates at level ξ_4; these are the scenarios 2, 4, and 6. Pedestrians with an awareness level ξ_4 consider the strategy of moving towards less crowded areas to avoid possible contagion, while still aiming to exit the room. Therefore, when more pedestrians apply this strategy, they have fewer chances of becoming exposed; this is exactly what happens in scenarios 2, 4, and 6. Conversely, scenarios with a majority of pedestrians that begin at level ξ_1, that is scenarios 1, 3, and 5, lead to an opposite situation. Since pedestrians with awareness level ξ_1 focus on finding the exit rather than avoiding densely populated areas, they become more vulnerable to contagion. Figure 4 demonstrates that this strategy significantly increases their chances of becoming exposed. Finally, scenarios 7 and 8 are analyzed, where 70% of pedestrians are initially equally distributed in the central awareness levels ξ_2 and ξ_3. In scenario 7, the remaining pedestrians are divided between 20% at awareness level ξ_1 and 10% at awareness level ξ_4. In contrast, scenario 8 initially has 10% of pedestrians at level ξ_1 and 20% at level ξ_4. Notably, despite the similar initial distributions, the results observed are similar to those in previous scenarios, reinforcing the finding that a higher percentage of pedestrians starting at the highest awareness level ξ_4 results in fewer exposed individuals and a shorter evacuation time.

Figure 4 also illustrates the impact of the awareness level on the evacuation time. Observe that scenario 6 (where all pedestrians have level ξ_4) achieves the shortest evacuation time, whereas scenario 5 (where all pedestrians have level ξ_1) results in the longest evacuation time. This difference is due to the opposite behavior tendencies. Pedestrians with level ξ_1 prioritize reaching the exit over avoiding congestion, leading to crowding and being forced to stop. In contrast, pedestrians with level ξ_4 actively seek less congested areas and maintain distance from others, allowing continuous movement. Figure 5 shows these contrasting behaviors during the evacuation process.

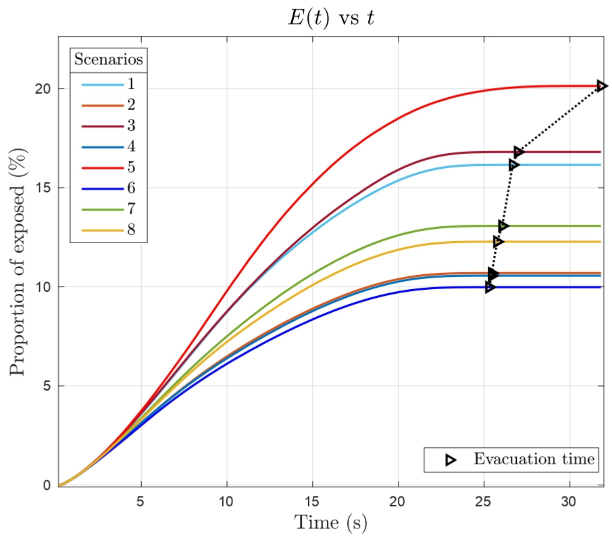

Figure 4. Evolution of the total number of exposed pedestrians over time. Each scenario indicates its evacuation time. Once completed, the number of exposed individuals remains constant until the evacuation of all scenarios is finished.

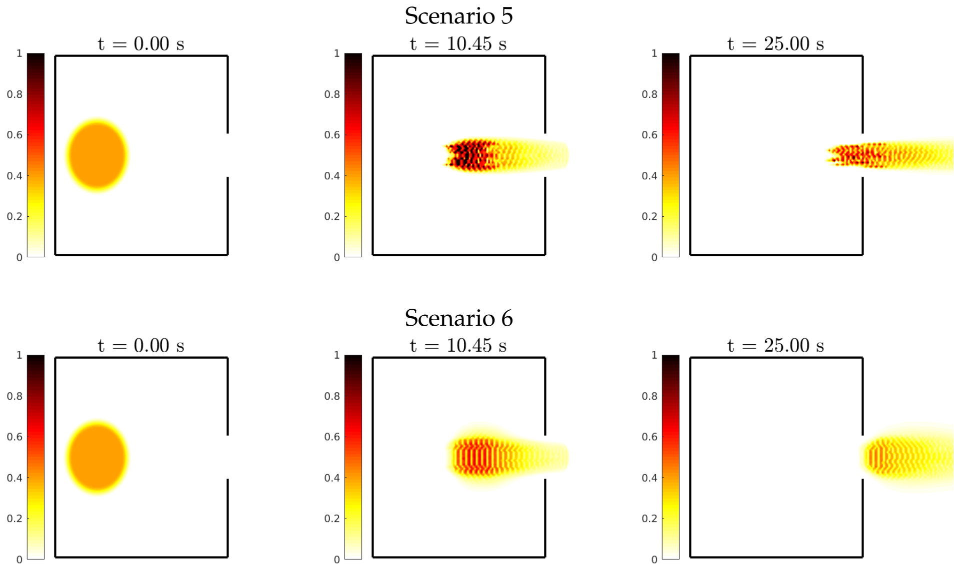

Figure 5. Evolution of the evacuation process for scenarios 5 and 6 from Case Study 1. In scenario 5 (**top** row), pedestrians focus on finding the exit and tend to crowd together. In scenario 6 (**bottom** row), pedestrians tend to look for less crowded paths.

To better understand the difference in the evacuation times, the changes in proportions of the different awareness levels over time are examined for each scenario. Recall that the total number of pedestrians with a given level of awareness level at time t is given by Equation (9). Figure 6 presents the results, revealing two key trends: (i) a symmetric pattern emerges between opposing scenarios, and (ii) a tendency towards intermediate awareness levels occurs. Specifically, scenario 1 starts with an initial high proportion of pedestrians in level ξ_1, but interactions among pedestrians during the evacuation process lead to a pronounced transition towards level ξ_2 (see Figure 6a). Similarly, scenario 2, where most pedestrians initially belong to ξ_4 exhibits a similar trend with interactions that drive pedestrians to the level ξ_3 (see Figure 6b). The same kind of behavior can be observed in scenarios 3 and 4 (Figure 6c,d) and scenarios 7 and 8 (Figure 6g,h). These tendencies towards the central levels occur because of the way in which the tables of games are defined. As discussed in Section 2.3, when pedestrians with different levels interact, there is a positive probability of moving closer by one level, but they cannot move further apart, resulting in a natural convergence towards the central levels. Regarding scenarios 5 and 6, no evolution in awareness levels is observed (see Figure 6e,f, respectively). This happens because the entire population belongs to a single level, so when pedestrians interact with others of the same level, the probability of staying in the same state is always 1, indicating no possibility of changing awareness levels.

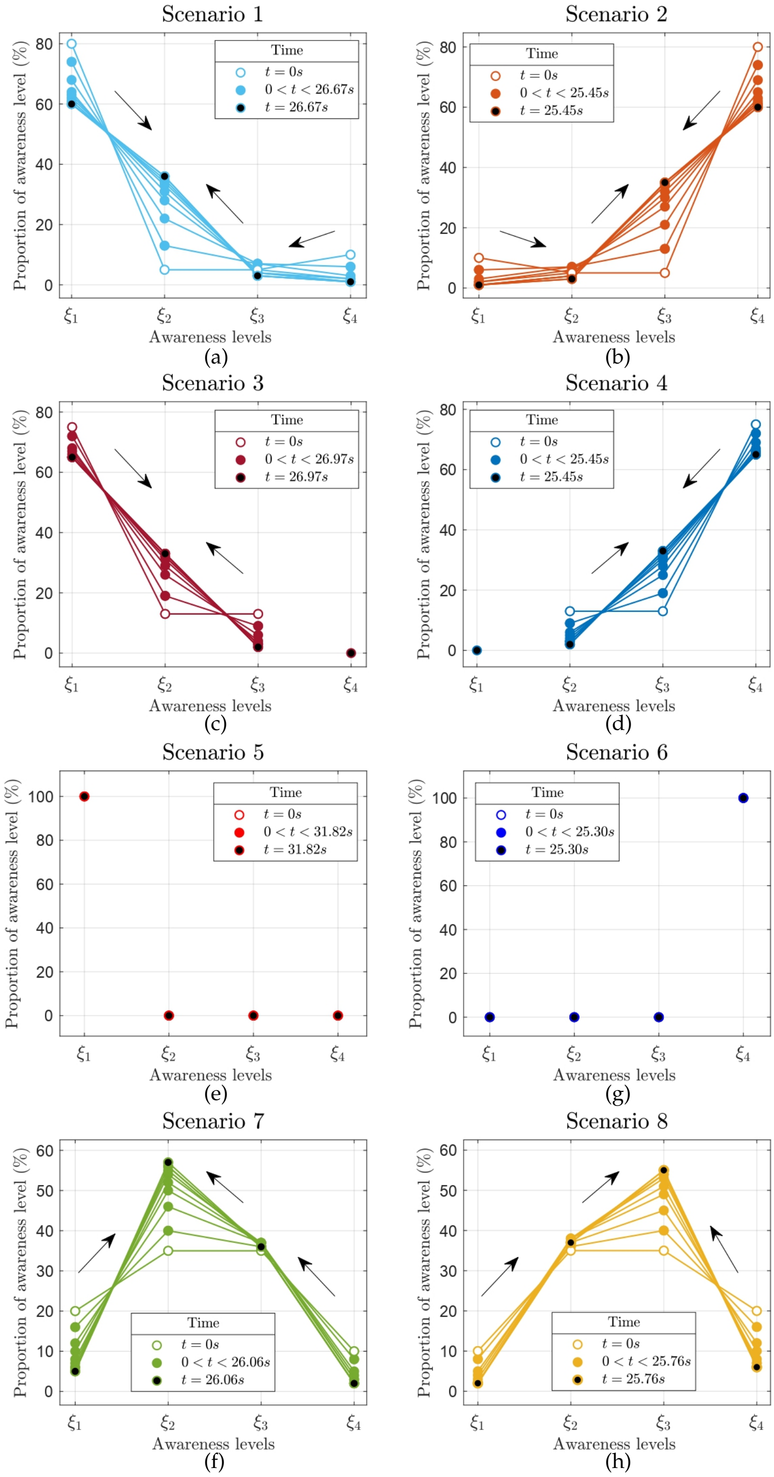

Figure 6. Evolution of the total number of pedestrians with a given level of awareness over time. Figures (**a**–**h**) correspond to scenarios 1–8, respectively. In each figure, the nodes represent the total number of pedestrians with awareness level ξ_k, for $k = 1, \ldots, 4$, at time t, given by (9). To show the evolution with respect to time t, the proportions of pedestrians at each level are connected by segments. The arrows indicate where the changes in the levels of awareness occur.

Finally, Figure 7 shows the evolution of the minimum velocity reached by pedestrians with respect to time for all the proposed scenarios. It can be seen that there is an indirect influence of awareness levels on the velocity modulus of pedestrians. In scenarios 1, 3, and 5 (Figure 7a–c), pedestrians (at least one) reach a minimum velocity of zero during almost the entire evacuation process. This phenomenon is interesting because if there was at least one pedestrian with zero velocity throughout the evacuation process, it means that at almost any time, at least one pedestrian had to stop due to the high density generated by congestion. This congestion is a consequence of the strategy of pedestrians to follow the main stream, heavily influenced by the level ξ_1, leading to overcrowding. Recall that these scenarios start with a vast majority of individuals at awareness level ξ_1.

On the other hand, in scenarios 2, 4, and 6 (see Figure 7a–c), the minimum velocity of pedestrians does not reach zero during the evacuation process. This indicates that pedestrians maintained movement throughout the evacuation, avoiding stops. These scenarios start with a vast majority of individuals at awareness level ξ_4. The underlying strategy of avoiding highly congested areas, strongly influenced by level ξ_4, enabled pedestrians to create and exploit low-crowding zones. By doing so, they were able to continue walking without interruptions, demonstrating the effectiveness of this strategy in preventing congestion.

Figure 7d presents the results of the intermediate scenarios 7 and 8. It is worth noting that both scenarios exhibit time intervals in which the velocity of pedestrians (at least of one) drops to zero. However, a comparison of the minimum velocities achieved reveals a significant difference: scenario 8, with 10% of pedestrians starting at awareness level ξ_4 always achieves a higher minimum velocity than scenario 7, where 20% begin at level ξ_1. This difference reinforces the influence of awareness level on the velocity modulus.

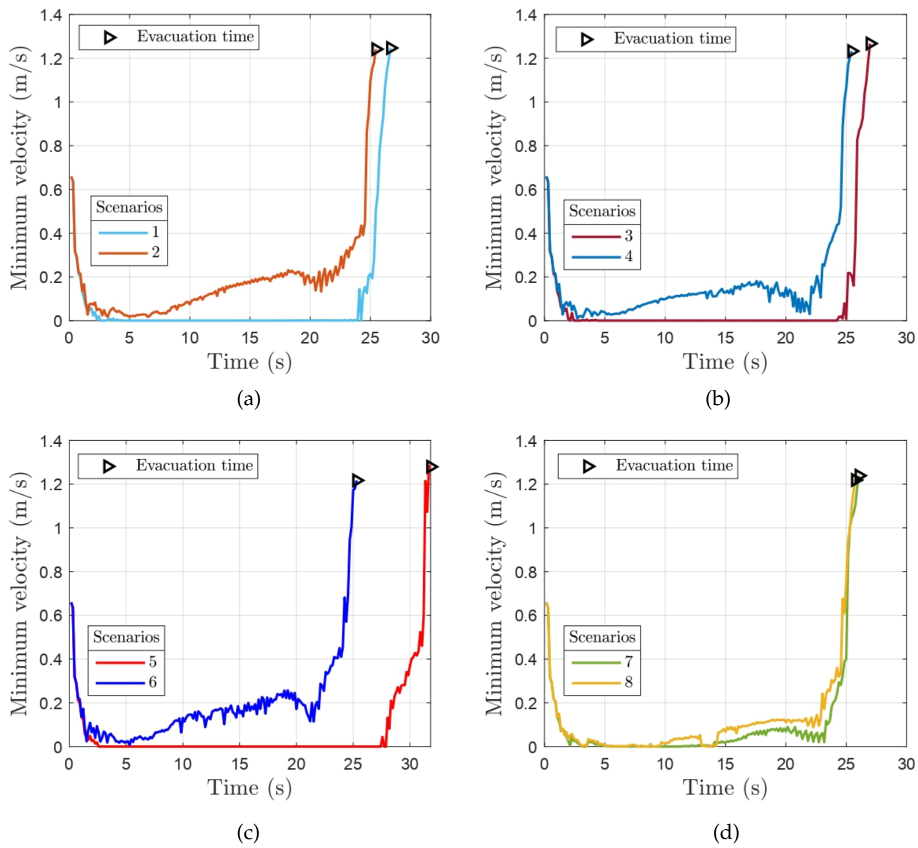

Figure 7. Evolution of the minimum velocity reached by pedestrians over time for the different scenarios of Case Study 1. Each figure (**a**–**d**) compares, each of them, two scenarios as specified in the legends.

Based on the previous results, it is concluded that the awareness level has a profound impact on the evacuation process. Initially, a significant influence on the spread of disease was observed. However, as various scenarios were explored, considerable effects on other factors, including the evacuation time and velocity modulus were also noted. The incorporation of awareness levels is a valuable contribution to our model as it provides a better representation of pedestrians' behavior and differentiates their strategies. Furthermore, this addition brings our model closer to simulating real-life situations.

3.2. Case Study 2: Awareness vs. Vaccination

This case study compares and contrasts *(i)* a population that is aware of contagion vs. *(ii)* a vaccinated population. The main question to answer is, 'Which microscopic state is the most effective in preventing massive spread: a high level of awareness or being vaccinated?'. This study is relevant in the context of public health strategies during pandemics, such as COVID-19, where both vaccination campaigns and awareness programs were crucial in controlling the spread of the virus. From this question, other points of interest arise, such as studying combinations of different populations, for example, a proportion of the population that is vaccinated but not aware, or determining which distribution of initial proportions results in the lowest number of exposed individuals. Understanding these dynamics can help optimize resource allocation and intervention strategies in future outbreaks. Table 2 shows the scenarios to be studied with their respective initial involved populations as well as the definition of the function ψ. Various initial proportions for susceptible S and vaccinated V pedestrians are considered for the different scenarios. However, in all scenarios, 50% of the pedestrians initially belong to the infectious compartment I. This choice aims to maximize the potential for disease contagion, enabling us to assess which state is more resilient against the spread of disease.

Table 2. Scenarios considered in Case Study 2. Initial proportions for infectious levels and awareness levels are shown, as well as the definition of function ψ.

Scenarios	Initial Proportion of Individuals (%) and Function ψ								
	S	I	E	V	ξ_1	ξ_2	ξ_3	ξ_4	$\psi(\xi)$
9	37.5	50	0	12.5	80	5	5	10	$1-\xi$
10	37.5	50	0	12.5	10	5	5	80	$1-\xi$
11	25	50	0	25	80	5	5	10	$1-\xi$
12	25	50	0	25	10	5	5	80	$1-\xi$
13	12.5	50	0	37.5	80	5	5	10	$1-\xi$
14	12.5	50	0	37.5	10	5	5	80	$1-\xi$

The results for the scenarios proposed in Table 2 are shown in Figure 8. Some very interesting results were obtained. Let us start with scenario 9, which performs the worst, as it shows the highest increase in the total number of exposed pedestrians at the end of the evacuation process and the largest decrease in the proportion of susceptible and vaccinated individuals, as shown in Figure 8a,b, respectively. The observed differences can be attributed to the initial population composition, characterized by a majority of pedestrians with awareness level ξ_1 and with a higher proportion of susceptible (but non-vaccinated) individuals compared to vaccinated ones. Conversely, scenario 14 presents a majority of individuals starting at awareness level ξ_4 and with a higher proportion of vaccinated individuals compared to susceptible (and non-vaccinated) ones. Moreover, a point to note is that the final proportion of exposed individuals does not exceed 5% of the total population for this scenario. These two scenarios represent the extreme cases, producing outcomes consistent with predictions.

Let us move on to understand the combined scenarios. Scenario 10 has an initial population with a lower proportion of vaccinated individuals but a higher proportion of pedestrians start at level ξ_4. However, this scenario presents a higher level of contagion compared to scenario 13, which has an initial proportion with a majority of individuals vaccinated and with awareness level ξ_1. The comparison between these two scenarios is important as it provides an initial answer to our main question: being vaccinated seems to be more effective than having a high awareness level in preventing the spread of a disease. This assertion can be reinforced by comparing scenarios 12 and 13, as the same pattern occurs: a higher proportion of vaccinated individuals results in a lower number of exposed individuals, even when most people initially belong to level ξ_1. It should be noted that the difference in the total number of pedestrians exposed at the end of the evacuation process between scenarios 12 and 13 is considerably smaller than that between scenarios 10 and 13.

An interesting comparison is between scenarios 10 and 11. As shown in Figure 8a, the curve describing the evolution of the total number of exposed pedestrians over time intersect for scenarios 10 and 11. The same happens for the curve representing the evolution of the total number of vaccinated and susceptible pedestrians (see Figure 8b). Recall that scenario 11 has the same initial number of vaccinated and susceptible (but non-vaccinated) individuals in the population and a majority of pedestrians starting at level ξ_1. Scenario 10 has an initial population with a lower proportion of vaccinated compared to susceptible (and non-vaccinated) pedestrians and a majority of individuals starting level ξ_4. Note that the curves in Figure 8a,b intersect at approximately 17 s. This intersection occurs because pedestrians are nearing the exit at that moment, generating a bottleneck (Figure 9). Pedestrians with awareness level ξ_1 or ξ_2 tend to crowd near the exit, causing an increase in contagion of the infectious disease, as observed in scenario 11. In contrast, pedestrians with awareness level ξ_3 or ξ_4 choose to distance themselves when approaching the exit, allowing a more fluid exit and reducing the number of infections, as seen in scenario 10.

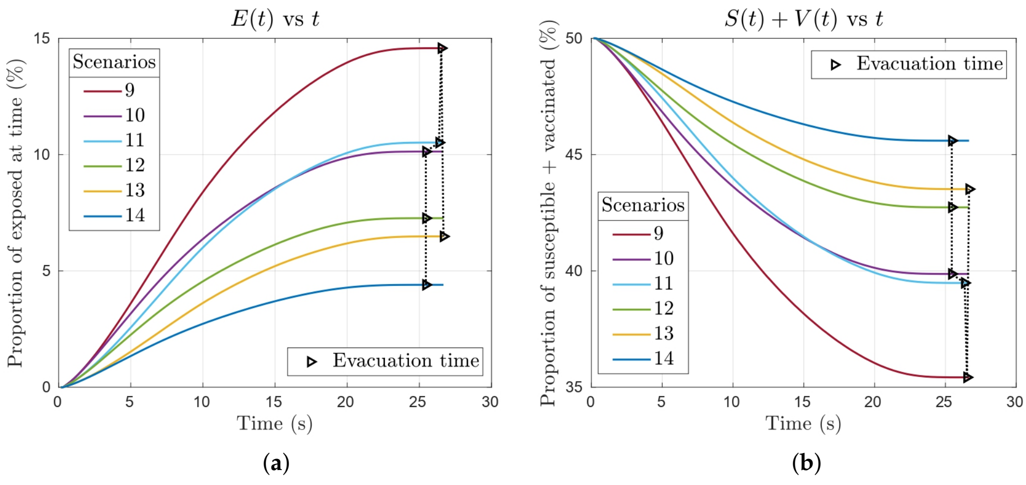

Figure 8. Results of Case Study 2. (**a**) Evolution of the total number of exposed pedestrians over time for each scenario. (**b**) Evolution of the total number of susceptible and vaccinated with respect to time for each scenario.

According to the obtained results, being vaccinated and having a high level of awareness are both important to help prevent the spread of a disease, but in the case of an evacuation from a closed domain through a narrow exit, the condition of being vaccinated seems to be more relevant.

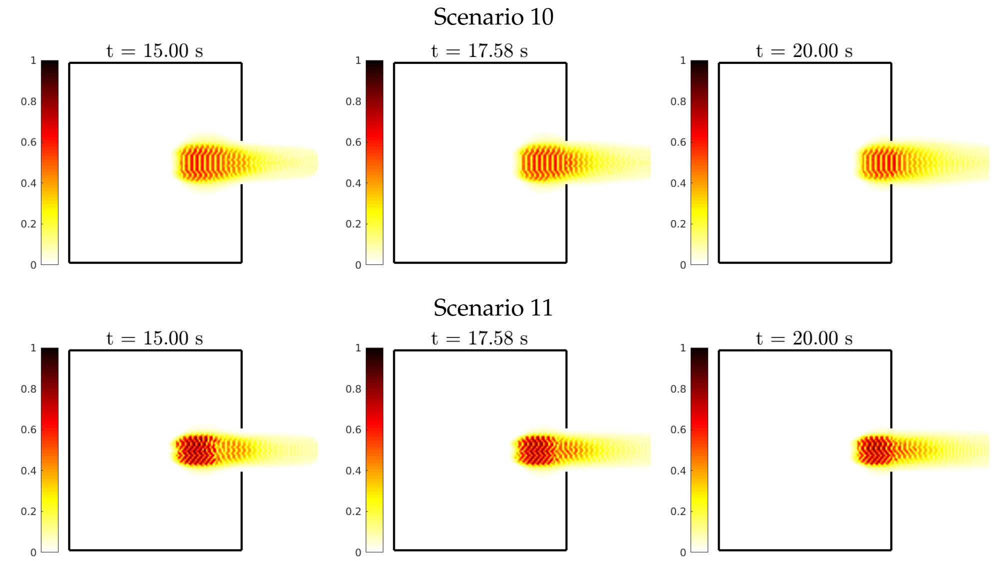

Figure 9. Evolution of the evacuation process for scenarios 10 and 11 from Case Study 2. In scenario 10 (**top** row), pedestrians tend to look for less crowded paths. In scenario 11 (**bottom** row), pedestrians focus on finding the exit and tend to crowd together, causing an increase in contagion of an infectious disease.

3.3. Case Study 3: Analyzing the Role of $\psi(\xi)$

This last case study focuses on understanding the role of the function ψ and its influence on the evacuation process. Recall that the values of this function reinforce the tendency to move towards less congested areas or, in contrast, reinforce the tendency to follow the stream, as seen in Equation (6). When infected individuals are moving within a behavioral crowd, understanding how people choose between following the crowd or seeking less congested routes can help optimize evacuation strategies to minimize both the evacuation time and the spread of infectious diseases. Understanding how the different choices of ψ affect or have an effect on the evacuation time and the spread of a disease is a key objective. Table 3 shows the nine scenarios to be studied.

Table 3. Scenarios considered in Case Study 3. Initial proportions for awareness levels and infectious levels as well as the definition of the different functions ψ to be considered.

Scenarios	**Initial Proportion of Individuals (%) and Function ψ**								
	$\psi(\xi)$	ξ_1	ξ_2	ξ_3	ξ_4	S	I	E	V
15	$1-\xi$	80	5	5	10	75	25	0	0
16	$1-\xi^2$	80	5	5	10	75	25	0	0
17	$1-\xi^3$	80	5	5	10	75	25	0	0
18	$1-\xi$	10	5	5	80	75	25	0	0
19	$1-\xi^2$	10	5	5	80	75	25	0	0
20	$1-\xi^3$	10	5	5	80	75	25	0	0
21	$1-\xi$	25	25	25	25	75	25	0	0
22	$1-\xi^2$	25	25	25	25	75	25	0	0
23	$1-\xi^3$	25	25	25	25	75	25	0	0

First, scenarios 15, 16, and 17 that end with the highest number of exposed individuals and longest evacuation times are analyzed (see Figure 10a). This behavior is attributed to the fact that in these scenarios, the majority of the initial population belongs to the awareness level ξ_1, and therefore, at least during the start of the evacuation, most pedestrians tend to follow the stream since $\psi(\xi_1)$ is equal to 1 (for all considered functions ψ). This behavior causes high congestion, facilitating contagion and also increasing the evacuation time. Furthermore, as the evacuation progresses, some pedestrians initially at awareness level ξ_1 transition to levels ξ_2 or ξ_3 (the vast majority will transition to ξ_2). For these individuals, the values of the different functions ψ differ. Specifically, the cubic function yields values closer to 1 at levels ξ_2 or ξ_3 compared to the quadratic and linear function. Consequently, pedestrians with awareness levels ξ_2 and ξ_3 have a stronger tendency to follow the stream when using the cubic function, whereas the linear function induces a weaker inclination to follow this behavior. This explains why, despite starting with the same initial population, scenarios 15, 16, and 17 end with differences in the evacuation time and in the total number of exposed individuals.

Next, scenarios 18, 19, and 20 exhibit the most favorable outcomes, with the lowest number of exposed individuals and shortest evacuation times (see Figure 10a). It is worth noting that the differences in evacuation time and final exposed pedestrians between these scenarios are less pronounced compared to the previous three. Specifically, scenarios 19 and 20 yield nearly identical results. This can be attributed to the majority of pedestrians starting at awareness level ξ_4, and for this level, the values of all functions ψ are equal. As time progresses, pedestrians transition to levels ξ_3 and ξ_2, mainly to ξ_3. Although the values of the different functions ψ in ξ_3 are different, they are all in the range $[0.3, 0.7]$ (see Figure 10b) and according to what was analyzed in [16], result in similar evacuation times (at least for a number of pedestrians like the one in this case study). In contrast, the values of the different functions in ξ_3 are in the range $[0.6, 1]$ (see Figure 10b), and according to what was analyzed in [16], this has a huge impact on the evacuation time, which reinforces the observations in the first three scenarios analyzed (scenarios 15, 16, and 17).

Finally, scenarios 21, 22, and 23 are examined to further understand the influence of the function ψ on the evacuation process. Recall that these scenarios assume that the initial proportions of pedestrians are evenly distributed across the levels of awareness. Figure 10 shows that scenario 23 is the one with the highest number of exposed individuals and longest evacuation times, while scenario 21 is the one with the lowest number of exposed individuals and the shortest evacuation time, among these three. This result can be attributed to the fact that the cubic function reinforces the tendency for pedestrians to follow the stream.

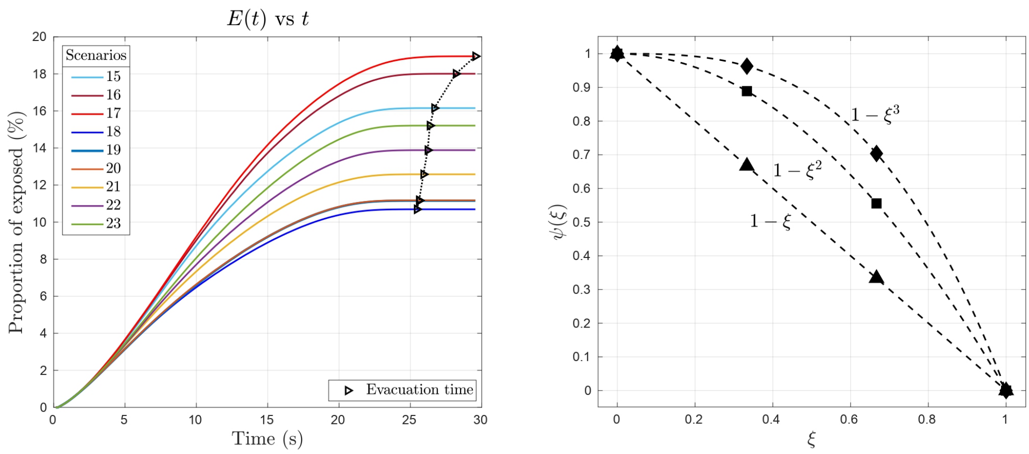

(**a**) (**b**)

Figure 10. Results of Case Study 3. (**a**) Evolution of the total number of exposed pedestrians over time for each scenario. (**b**) The three different functions ψ are considered. The values of the linear, quadratic, and cubic functions at awareness levels ξ_k, $k = 1, \ldots, 4$ are represented by triangles, squares, and diamonds, respectively.

Based on the previous results, it is concluded that when the function ψ takes values close to 1 at awareness levels ξ_k, it significantly increases the tendency for individuals to follow the stream, leading to congestion and an environment favorable to spread of the contagious disease. In contrast, when ψ values fall within the range $[0.3, 0.7]$, the tendency to follow the crowd decreases, resulting in a more fluid evacuation process.

4. Discussion and Conclusions

This study presents an extended kinetic model to analyze the dynamics of social crowds in the presence of an infectious disease, incorporating a novel variable for contagion awareness. The impact of awareness levels on evacuation times and contagion spread is investigated through three case studies. Our findings highlight several key points:

- **Impact of awareness on disease spread**: High levels of awareness significantly reduce the spread of disease. Individuals with high awareness adhere to social distancing, exhibit caution for themselves and others, and possess knowledge about safety and prevention measures. Conversely, low levels of awareness lead to greater disease propagation due to neglect of social distancing, indifference, and lack of knowledge. This finding is consistent with earlier results showing how stress or contagion awareness can shape crowd flow patterns [18,19]. A key contribution of this model is its ability to relate crowd dynamics to contagion spread.
- **Awareness evolution**: Pedestrians cannot independently evolve their awareness levels. In our model, the only way to transition to a different awareness state is through interactions with other pedestrians. This aligns with the findings of Kim and Quaini [17], who modeled emotional states (specifically fear) as continuous variables evolving over time. Unlike their model, where fear levels can change even if the entire population starts with the same level, our model shows that a population with uniform awareness levels remains static. The inclusion of a time-evolving awareness variable is motivated by the recent paper [18], where the authors emphasized the importance of advancing beyond models with fixed assumptions about pedestrian behavior. The present model confirms that conclusion.
- **Impact of awareness on the evacuation dynamics**: Unexpectedly, evacuation times were shorter for scenarios with high awareness levels. The initial assumption was that low-awareness pedestrians, focused solely on exiting the room, would achieve faster evacuation by reaching their maximum allowed speed. However, high-awareness pedestrians, by maintaining social distance, actually evacuated more efficiently. This counterintuitive result is explained by the function ψ, which influences the evacuation dynamics. Our results are consistent with Agnelli et al. [16], who found that an optimal parameter value of $\varepsilon = 0.4$ minimized the evacuation time. In our study, low-awareness pedestrians had ε values close to 1, while high-awareness pedestrians had values near 0. There are some practical applications to this counterintuitive result. For instance, during the COVID-19 crisis, some airlines implemented a system to deplane by rows to prevent contagion, resulting in shorter disembarking times (some interesting models can be found in [30–32]). In the same context, Kim and Quaini [33] simulated passengers in an airport terminal under the simplifying assumption that walking velocity was predetermined. A major strength of our model is that it eliminates this assumption, allowing for more realistic simulations
- **Action of vaccination**: Interesting insights into the action of vaccination were also obtained. In a situation in which there is no available immunization to an infectious disease, it is evident that awareness must be promoted across the population. However, our results show that the existence of a vaccine can guarantee safety, allowing for the

relaxation of some policies related to contagion awareness (e.g., social distancing or use of masks), in agreement with well-accepted results in the field [2,3].

While our model provides valuable insights into crowd dynamics, evacuation processes, and contagion awareness, it is important to acknowledge its limitations. One key limitation is that the model relies on certain parameters that may vary significantly across different environments, populations, and diseases. Additionally, the assumption of discrete awareness levels may not fully capture the diversity of responses in real-world scenarios. Future work should aim to analyze, and eventually incorporate, continuous behavior patterns [17] and validate the model against a wider range of empirical data [21].

Addressing these limitations, future research should explore the impact of mixed populations with different awareness levels.

Moreover, extending the model to include vaccination strategies alongside awareness measures could offer a comprehensive understanding of their combined effects on disease spread and evacuation efficiency.

Despite these areas for improvement, our findings offer a robust framework for understanding the interplay between crowd behavior and disease spread. By addressing these limitations and pursuing the suggested future research directions, our model can be further refined to enhance its applicability to real-world situations, ultimately contributing to more effective public health policies and emergency response strategies.

Author Contributions: Conceptualization, J.P.A. and D.A.K.; methodology, J.P.A., C.A. and D.A.K.; software, C.A.; validation, J.P.A., C.A. and D.A.K.; formal analysis, J.P.A., C.A. and D.A.K.; investigation, J.P.A., C.A. and D.A.K.; resources, J.P.A., C.A. and D.A.K.; data curation, J.P.A., C.A. and D.A.K.; writing—original draft preparation, J.P.A., C.A. and D.A.K.; writing—review and editing, J.P.A., C.A. and D.A.K.; visualization, C.A.; supervision, J.P.A. and D.A.K.; project administration, J.P.A.; funding acquisition, J.P.A.and D.A.K. All authors have read and agreed to the published version of the manuscript.

Funding: This research was funded by Agencia Nacional de Promoción de la Investigación, el Desarrollo Tecnológico y la Innovación Project PICT 2021-0188, and SeCyT-UNC Project Formar 2023—33820230100083CB. D.K. is supported by Grant PID2023-146872OB-I00 financed by MICIU/AEI/10.13039.501100011033 and by Feder, EU.

Data Availability Statement: The original contributions presented in this study are included in the article. Further inquiries can be directed to the corresponding author.

Conflicts of Interest: The authors declare no conflicts of interest.

References

1. Zhu, Q.; Gao, Y.; Hu, Q.; Hu, D.; Wu, X. A study on the factors influencing the intention to receive booster shots of the COVID-19 vaccine in China based on the information frame effect. *Front. Public Health* **2024**, *12*, 1258188. [CrossRef] [PubMed]
2. Bellomo, N.; Bingham, R.; Chaplain, M.A.; Dosi, G.; Forni, G.; Knopoff, D.A.; Lowengrub, J.; Twarock, R.; Virgillito, M.E. A multiscale model of virus pandemic: Heterogeneous interactive entities in a globally connected world. *Math. Model. Methods Appl. Sci.* **2020**, *30*, 1591–1651. [CrossRef] [PubMed]
3. Aguiar, M.; Dosi, G.; Knopoff, D.A.; Virgillito, M.E. A multiscale network-based model of contagion dynamics: heterogeneity, spatial distancing and vaccination. *Math. Model. Methods Appl. Sci.* **2021**, *31*, 2425–2454. [CrossRef]
4. Wang, Q.; Jiang, Q.; Yang, Y.; Pan, J. The burden of travel for care and its influencing factors in China: an inpatient-based study of travel time. *J. Transp. Health* **2022**, *25*, 101353. [CrossRef]
5. Fan, Z.; Liu, Y.; Ye, Y.; Liao, Y. Functional probes for the diagnosis and treatment of infectious diseases. *Aggregate* **2024**, *5*, e620. [CrossRef]
6. Agnelli, J.P.; Buffa, B.; Knopoff, D.; Torres, G. A spatial kinetic model of crowd evacuation dynamics with infectious disease contagion. *Bull. Math. Biol.* **2023**, *85*, 23. [CrossRef]
7. Bellomo, N.; Brezzi, F.; Soler, J. Active particles methods and challenges in behavioral systems. *Math. Model. Methods Appl. Sci.* **2020**, *30*, 653–658. [CrossRef]

8. Bellomo, N.; Outada, N.; Soler, J.; Tao, Y.; Winkler, M. Chemotaxis and cross-diffusion models in complex environments: Models and analytic problems toward a multiscale vision. *Math. Model. Methods Appl. Sci.* **2022**, *32*, 713–792. [CrossRef]
9. Bellouquid, A.; Delitala, M. *Modelling Complex Biological Systems—A Kinetic Theory Approach*; Birkäuser: Boston, MA, USA, 2006.
10. Bellomo, N.; Ha, S.Y.; Outada, N.; Yoon, J. On the mathematical theory of behavioral swarms emerging collective dynamics. *Math. Model. Methods Appl. Sci.* **2022**, *32*, 2927–2959. [CrossRef]
11. Hartwell, L.H.; Hopfield, J.J.; Leibler, S.; Murray, A.W. From molecular to modular cell biology. *Nature* **1999**, *402*, C47–C52. [CrossRef]
12. Herrero, M.A. On the role of mathematics in biology. *J. Math. Biol.* **2007**, *54*, 887. [CrossRef] [PubMed]
13. May, R.M. Uses and abuses of mathematics in biology. *Science* **2004**, *303*, 790–793. [CrossRef] [PubMed]
14. Bellomo, N.; Burini, D.; Outada, N. Multiscale models of Covid-19 with mutations and variants. *Netw. Heterog. Media* **2022**, *17*, 293–310. [CrossRef]
15. Kim, D.; Quaini, A. Coupling kinetic theory approaches for pedestrian dynamics and disease contagion in a confined environment. *Math. Model. Methods Appl. Sci.* **2020**, *30*, 1893–1915. [CrossRef]
16. Agnelli, J.P.; Colasuonno, F.; Knopoff, D. A kinetic theory approach to the dynamics of crowd evacuation from bounded domains. *Math. Model. Methods Appl. Sci.* **2015**, *25*, 109–129. [CrossRef]
17. Kim, D.; O'Connell, K.; Ott, W.; Quaini, A. A kinetic theory approach for 2D crowd dynamics with emotional contagion. *Math. Model. Methods Appl. Sci.* **2021**, *31*, 1137–1162. [CrossRef]
18. Gibelli, L.; Knopoff, D.; Liao, J.; Yan, W. Macroscopic modeling of social crowds. *Math. Model. Methods Appl. Sci.* **2024**, *34*, 1135–1151. [CrossRef]
19. Knopoff, D.; Liao, J.; Ma, Q.; Yang, X. Individual-based crowd dynamics with social interaction. *Math. Model. Methods Appl. Sci.* **2025**, *in press.*
20. Bellomo, N.; Gibelli, L.; Quaini, A.; Reali, A. Towards a mathematical theory of behavioral human crowds. *Math. Model. Methods Appl. Sci.* **2022**, *32*, 321–358. [CrossRef]
21. Kim, D.; Labate, D.; Mily, K.; Quaini, A. Data driven learning to enhance a kinetic model of distressed crowd dynamics. *arXiv* **2024**, arXiv: 2411.12974.
22. Bellomo, N.; Dolfin, M.; Liao, J. Life and self-organization on the way to artificial intelligence for collective dynamics. *Phys. Life Rev.* **2024**, *51*, 1–8. [CrossRef]
23. Kim, D.; Quaini, A. A kinetic theory approach to model pedestrian dynamics in bounded domains with obstacles. *Kinet. Relat. Model.* **2019**, *12*, 1273–1296. [CrossRef]
24. Holden, H.; Karlsen, K.H.; Lie, K.A. *Splitting Methods for Partial Differential Equations with Rough Solutions: Analysis and MATLAB Programs*; European Mathematical Society—EMS Publishing House Zürich: Zurich, Switzerland, 2010.
25. LeVeque, R.J. *Finite Volume Methods for Hyperbolic Problems (Cambridge Texts in Applied Mathematics)*; Cambridge University Press: Cambridge, UK, 2002.
26. Piccoli, B.; Tosin, A. Time-evolving measures and macroscopic modeling of pedestrian flow. *Arch. Ration. Mech. Anal.* **2011**, *199*, 707–738. [CrossRef]
27. Schäfer, M. *Computational Engineering: Introduction to Numerical Methods*; Springer: Berlin/Heidelberg, Germany, 2006.
28. Buchmueller, S.; Weidmann, U. *Parameters of Pedestrians, Pedestrian Traffic and Walking Facilities*; IVT-Report Nr. 132, Institut for Transport Planning and Systems (IVT); Swiss Federal Institute of Technology Zurich (ETHZ): Zurich, Switzerland, 2006.
29. The MathWorks Inc. *MATLAB version: 23.2.0 (R2023b)*; The MathWorks Inc.: Natick, USA, 2023.
30. Schultz, M.; Fuchte, J. Evaluation of aircraft boarding scenarios considering reduced transmissions risks. *Sustainability* **2020**, *12*, 5329. [CrossRef]
31. Schultz, M.; Soolaki, M.; Bakhshian, E.; Salary, M.; Fuchte, J. COVID-19: Passenger boarding and disembarkation. In Proceedings of the Fourteenth USA/Europe Air Traffic Management Research and Development Seminar (ATM2021), Virtual, 20–23 September 2021.
32. Xie, C.Z.; Tang, T.Q.; Hu, P.C.; Huang, H.J. A civil aircraft passenger deplaning model considering patients with severe acute airborne disease. *J. Transp. Saf. Secur.* **2022**, *14*, 1063–1084. [CrossRef]
33. Kim, D.; Quaini, A. A kinetic theory approach to model crowd dynamics with disease contagion. In *Crowd Dynamics, Volume 3: Modeling and Social Applications in the Time of COVID-19*; Springer: Berlin/Heidelberg, Germany, 2021; pp. 157–183.